blood advances

American Society of Hematology
2021 L Street NW, Suite 900,
Washington, DC 20036
Phone: 202-776-0544 | Fax 202-776-0545
bloodadvances@hematology.org

Peripheral human red blood cell development in human immune system mouse model with heme oxygenase-1 deficiency

Tracking no: ADV-2023-011754R2

Aditi Patel (Regeneron Pharmaceuticals, Inc., United States) Kyle Trageser (Regeneron Pharmaceuticals, Inc., United States) Hyunjin Kim (Regeneron Pharmaceuticals, Inc., United States) Wei Keat Lim (Regeneron Pharmaceuticals, Inc., United States) Christina Adler (Regeneron Pharmaceuticals, Inc., United States) Brace Porter (Regeneron Pharmaceuticals, Inc., United States) Min Ni (Regeneron Pharmaceuticals, Inc., United States) Yi Wei (Regeneron Pharmaceuticals, United States) Gurinder Atwal (Regeneron Pharmaceuticals, Inc., United States) Parnian Bigdelou (Regeneron Pharmaceuticals, Inc., United States) Vikas Kulshreshtha (Regeneron Pharmaceuticals, Inc., United States) Dharani Ajithdoss (Regeneron Pharmaceuticals, Inc., United States) Jun Zhong (Regeneron Pharmaceuticals, Inc., United States) Naxin Tu (Regeneron Pharmaceuticals, Inc., United States) Lynn Macdonald (Regeneron, United States) Andrew Murphy (Regeneron Pharmaceuticals, Inc., United States) Davor Frleta (Regeneron Pharmaceuticals, Inc., United States)

Abstract:
A challenge for human immune system (HIS) mouse models has been the lack of human red blood cells (hRBCs) survival after engraftment of these immune-deficient mice with human CD34+ hematopoietic stem cells (HSCs). This limits the use of HIS models for preclinical testing of targets directed at hRBCs-related diseases. Even though human white blood cells can develop in the peripheral blood of these human HSC-engrafted mice, peripheral hRBCs are quickly phagocytosed by murine macrophages upon egress from the bone marrow (BM). Genetic ablation of murine myeloid cells results in severe pathology in resulting mice, rendering such an approach to increase hRBC survival in HIS mice impractical. Heme oxygenase-1 (HMOX-1) deficient mice have reduced macrophages due to toxic build-up of intracellular heme upon engulfment of red blood cells, but do not have an overall loss of myeloid cells. We took advantage of this observation and generated a HMOX-1-/- on a humanized M-CSF/SIRPa/CD47 Rag2-/- IL-2Rg-/- background. These mice have reduced murine macrophages but comparable level of murine myeloid cells to HMOX-1+/+ control mice in the same background. Injected hRBCs survive longer in HMOX-1-/- mice than in HMOX-1+/+ controls. Additionally, upon human HSC-engraftment, hRBCs can be observed in the peripheral blood of HMOX-1-/- humanized M-CSF/SIRPa/CD47 Rag2-/- IL-2Rg-/- mice and hRBC levels can be increased by treatment with human erythropoietin. Since hRBC are present in the peripheral blood of engrafted HMOX-1-/- mice, these mice have the potential to be used for hematological disease modeling, and to test therapeutic treatments for hRBC diseases in vivo.

Conflict of interest: COI declared - see note

COI notes: All authors are current or former employees of Regeneron Pharmaceuticals Inc. and may hold stock and/or stock options in the company. D.F. and N.T. are inventors on a pending U.S. patent application no. 18/223,434 entitled "Genetically modified non-human animals and methods of use thereof."

Preprint server: No;

Author contributions and disclosures: A.K.P. and K.T. engrafted mice and performed experiments. H.K. and W.K.L. analyzed molecular profiling data. C.A. and S.P. prepared samples for single-cell RNAseq. M.N., Y.W., and G.S.A. provided guidance on molecular profiling of mouse and human samples. P.B. performed serum chemistry analysis. V.K. and D.A. analyzed histology. J.Z. managed mouse husbandry and establishment of the MSRG47 HMOX-1-/- mouse line. N.T. designed the HMOX-1 deletion to be cloned and targeted. L.M. and A.M. provided support and guidance on this project. D.F. developed the idea in using HMOX-1 deficient mice for hRBC survival, led the project, and wrote the manuscript.

Non-author contributions and disclosures: No;

Agreement to Share Publication-Related Data and Data Sharing Statement: All data generated or analyzed during this study are included in this published article. Single-cell RNAseq data reported here has been deposited in Gene Expression Omnibus. The accession code is GSE239736. Please reach out to corresponding author for any material requests.

Clinical trial registration information (if any):

Peripheral human red blood cell development in human immune system mouse model with heme oxygenase-1 deficiency

Human RBCs persist in heme oxygenase-1 deficient mice

Aditi Khatri Patel[1], Kyle Trageser[1], Hyunjin Kim[1], Wei keat Lim[1], Christina Adler[1], Brace Porter[1], Min Ni[1], Yi Wei[1], Gurinder S. Atwal[1], Parnian Bigdelou[1], Vikas Kulshreshtha[1], Dharani Ajithdoss[1], Jun Zhong[1], Naxin Tu[1], Lynn Macdonald[1], Andrew Murphy[1], Davor Frleta[1,2]

[1]Regeneron Pharmaceuticals, Inc. 795 Old Saw Mill River Road Tarrytown, NY 10591

[2]Corresponding author: Regeneron Pharmaceuticals, Inc. 795 Old Saw Mill River Road, Suite 92-106, Tarrytown, NY 10591. 914-847-7113

Davor.Frleta@regeneron.com

Data sharing statement: All data generated or analyzed during this study are included in this published article. Single-cell RNAseq data reported here has been deposited in Gene Expression Omnibus. The accession code is GSE239736.

Please reach out to corresponding author for any material requests.

Word counts

Abstract/Text: 5,205

Figures: 1,031

References: 1,152

Key points

- Immuno-deficient mice with murine heme oxygenase-1 deletion allow persistence of human red blood cells (hRBCs) in their peripheral blood.
- Immuno-deficient mice with murine heme oxygenase-1 deletion have reduced erythrophagocytic macrophages.

Abstract

A challenge for human immune system (HIS) mouse models has been the lack of human red blood cells (hRBCs) survival after engraftment of these immune-deficient mice with human CD34+ hematopoietic stem cells (HSCs). This limits the use of HIS models for preclinical testing of targets directed at hRBCs-related diseases. Even though human white blood cells can develop in the peripheral blood of these human HSC-engrafted mice, peripheral hRBCs are quickly phagocytosed by murine macrophages upon egress from the bone marrow (BM). Genetic ablation of murine myeloid cells results in severe pathology in resulting mice, rendering such an approach to increase hRBC survival in HIS mice impractical. Heme oxygenase-1 (HMOX-1) deficient mice have reduced macrophages due to toxic build-up of intracellular heme upon engulfment of red blood cells, but do not have an overall loss of myeloid cells. We took advantage of this observation and generated a HMOX-$1^{-/-}$ on a humanized M-CSF/SIRPα/CD47 Rag2-/- IL-$2R_{\gamma}$-/- background. These mice have reduced murine macrophages but comparable level of murine myeloid cells to HMOX-$1^{+/+}$ control mice in the same background. Injected hRBCs survive longer in HMOX-$1^{-/-}$ mice than in HMOX-$1^{+/+}$ controls. Additionally, upon human HSC-engraftment, hRBCs can be observed in the peripheral blood of HMOX-$1^{-/-}$ humanized M-CSF/SIRPα/CD47 Rag2-/- IL-$2R_{\gamma}$-/- mice and hRBC levels can be increased by treatment with human erythropoietin. Since hRBC are present in the peripheral blood of

engrafted HMOX-1$^{-/-}$ mice, these mice have the potential to be used for hematological disease modeling, and to test therapeutic treatments for hRBC diseases in vivo.

Introduction

Immuno-deficient mouse models engrafted with a human immune system (HIS mice) are attractive platforms for preclinical testing of novel therapeutics, disease modeling, and studying basic human immuno-biology. HIS mice are engrafted with human CD34+ hematopoietic stem cells (HSCs) that give rise to human T cells, B cells, NK cells, dendritic cells, granulocytes, and myeloid cells in HIS mice[1-4]. These models have allowed testing of potential reagents directed at human leukocytes such as T cell activating reagents (e.g. checkpoint inhibitors)[5,6], B cell depleting antibodies[4,7-9], and pharmacological mobilizers of HSCs[10-12]. Additionally, HIS mice can be used for various disease modeling[13-15].

HIS mice engrafted with HSCs do not have human red blood cells (hRBCs) present in the blood despite developing from HSCs. Immature human reticulocytes can develop in the bone marrow (BM) of HIS mice, but they are rapidly destroyed upon egress from the BM[16]. Injection of hRBCs into non-engrafted immune-deficient mice demonstrates that hRBCs are quickly cleared from the peripheral blood, usually within hours of injection[16]. Murine macrophages are responsible for clearance of hRBCs from peripheral blood[16-18]. Treatment of HIS mice with clodronate liposomes that temporarily deplete macrophages leads to emergence of hRBCs in the peripheral blood of HIS mice as well as prolongs injected hRBCs in the blood[16,17].

Prolonged removal of murine macrophages from HIS models is fraught with difficulty. Repeated injection of clodronate liposomes is not feasible due to murine toxicity. Genetic modifications that ablate murine myeloid development also negatively impact mouse development. For example, mice with a deletion of the *CSF1R* gene, the receptor for M-CSF which is critical for myeloid cell development, have severe skeletal pathology and usually die before weaning[19]. This is due to a loss of osteoclasts, a subset of myeloid cells that consume bone and work in balance with osteoblasts to shape BM[20-22]. Since human HSC engraftment relies on hematopoiesis in the BM, HSC engraftment would be perturbed in mice lacking a BM which would impede leukopoiesis as well as erythropoiesis. Thus, hRBC survival requires a HIS mouse model with a loss of murine macrophages (phagocytic cells) but not a complete loss of all murine myeloid cell subsets.

Heme oxygenase-1 (HMOX-1) is an inducible enzyme that processes heme from internalized RBCs to release and recycle iron[23]. A deficiency in human HMOX-1 was reported in a patient that died at 6 years of age[24,25]. The patient suffered from growth retardation, severe anemia, as well as fibrosis of spleen, liver, and kidney. Due to disruption in iron recycling, iron deposition resulted in damage to liver and kidney[24,25]. HMOX-1$^{-/-}$ mice exhibited similar pathology as the HMOX-1-deficient patient[23,26]. HMOX-1$^{-/-}$ mice develop anemia and iron overload in their kidney and liver[20,23,26,27]. They also exhibit growth retardation and even though they initially have splenomegaly, the mice develop splenic fibrosis as they age[26,28]. Because of these pathologies, HMOX-1$^{-/-}$ mice have reduced survival[26,28].

HMOX-1$^{-/-}$ mice lack macrophages in both spleen, liver, and BM due to toxic intracellular build-up of heme within macrophages that engulf RBCs[26,27,29]. Normally, phagocytosis of senescent RBCs by erythrophagocytic macrophages is necessary for clearance of

dying RBCs and recycling of iron[26,29]. HMOX-1-deficiency disrupts this process resulting in pathological iron overload in the kidney and liver[26,27,29]. Treating HMOX-1$^{-/-}$ macrophages with RBCs in vitro induces cellular death[26]. The lack of macrophages necessary for iron recycling is believed to be the primary cause of pathology in HMOX-1$^{-/-}$ as transfer of WT BM ameliorates disease pathology in HMOX-1$^{-/-}$ mice[29,30].

Despite a loss of erythrophagocytic macrophages, HMOX-1$^{-/-}$ mice still have CD11b+ myeloid cells[26,27]. In accordance with still having CD11b+ myeloid cells, HMOX-1$^{-/-}$ mice do not exhibit skeletal pathology as do CSF1R$^{-/-}$ mice[19,26,28]. Furthermore, HMOX-1$^{-/-}$ in an immune-deficient background are healthier than counterparts in an immune-competent background, as noted by a lack of liver and kidney fibrosis as well as serum indicators of liver and kidney health. The loss of macrophages that engulf RBCs, but not the concomitant loss of all myeloid cell subsets, made HMOX-1 deficiency an attractive approach to rescue hRBCs developing in human HSC-engrafted HIS mice.

We show here that when we deleted HMOX-1 in our immune-deficient mice (hSIRPα/hM-CSF/hCD47/Rag2$^{-/-}$/IL-2Rγ$^{-/-}$ HIS mice), this allows for survival of hRBCs with either passively injected hRBCs or human HSC engraftment of the mice.

Methods

Mice

For generation of HMOX-1$^{-/-}$ mice, mouse Hmox1 gene was knocked out in the mouse genome using VELOCIGENE® technology, an approximately 7kb mouse genomic sequence of Hmox1 gene from the start codon ATG to the stop codon, was deleted on mouse chromosome 8 C1, between coordinates chr8: 75093750-75100019 (GRCm38 assembly). To make the targeting vector from mouse BAC clone RP23-102I24 by the BHR step, a Hygromycin (Hyg) resistance self-del cassette (with CRE recombinase controlled by Protamine promoter) flanked by lox sites (lox2372-hyg-lox2372), to replace ~7 kb mouse sequence containing the mouse Hmox1 gene. Mouse homology arms were made by PCR amplification using BAC clone RP23-102I24 as the template, 5' Homology Arm by 5' primer: GATGTTGCAACAGCAGCGAGAA and 33' primer: CACCGGACTGGGCTAGTTCA; 3' Homology Arm by 5' primer: ATGCAATACTGGCCCCCAGG and 3' primer: GATTTGGGGCTGCTGGTTTCAA.

The final targeting vector contained from 5' to 3': the chloramphenicol resistance cassette (CM), the 5' mouse homology arm, the lox2372-Hyg-lox2372 self-del cassette, the 3' mouse homology arm, the final clone was selected based on CM/Hyg resistance, which targeting vector was

electroporated into mouse embryonic stem (ES) cells with humanized SIRPα, humanized M-CSF, humanized CD47 and Rag2-/- IL-2Rγ-/-. Targeted homologous recombination resulted in deletion of ~7 kb of mouse sequence (GRCm38 coordinates chr8: 75093750-75100019). Successful integration was confirmed by a modification of allele (MOA) assay. Primers and probes used for the MOA assay for the loss of mouse Hmox1 sequences by Hmox1_U Probe (TCAGACGATTTGTAAGATGCAGGGA) and Hmox1_D Probe (TGTAGCAGATCCTGGCCTTGGAC).

The mouse embryo comprising the donor ES cells was incubated in vitro and then implanted into a surrogate mother to produce an F0 mouse fully derived from the donor ES cells. Mice with Hmox1 gene deleted were identified by genotyping using the MOA assay described above. Mice heterozygous for KO Hmox1 gene were bred to homozygosity . Mice were maintained on a sulfa diet (LabDiet, St. Louis, MO) in a MPF facility, and were intra-bred for about 5-10 generations. All experiments were done in compliance with Regeneron Institutional Animal Care and Use Committee protocols. Human fetal liver (FL) samples used for isolating human CD34+ HSCs were obtained from Advanced Biosciences Resources (Alameda, CA) with proper consent

Passive transfusion of hRBCs

In non-engrafted HMOX-1$^{+/+}$ and HMOX-1$^{-/-}$ hSIRPα/hM-CSF/hCD47/Rag2$^{-/-}$/IL-2Rγ$^{-/-}$ mice, 4x10^{7} hRBCs were injected intra-peritoneally (n=7 per mouse strain). Mice were bled daily until Day 8 post-injection and blood collected in PBS + 5mM EDTA for counting and FACS analysis.

Human CD34+ Cell Isolation

Human fetal liver (FL) samples were obtained from Advanced Biosciences Resources (Alameda, CA) with proper consent. FL samples were cut in small fragments, treated for 25 min at 37°C with Collagenase D (100ng/mL; Roche). Cell suspension was prepared and the human CD34+ cells were separated by density gradient centrifugation, followed by positive immunomagnetic selection using anti-human CD34 microbeads according to the manufacturer's instructions (Miltenyi Biotec). Cells were either frozen in 10% DMSO containing human albumin serum and kept in liquid nitrogen or injected directly.

Human CD34+ Immune Cell Reconstitution

Newborn pups were sublethally irradiated (160 cGy; X-RAD 320 irradiator) 4-24 hours prior to an intrahepatic injection of $1x10^5$ human FL-derived CD34+ cells.

Analysis of Human Hematopoietic Cell Populations

For analyzing hRBC populations, blood was collected in PBS + 5mM EDTA and counted using a Beckman-Coulter counter. Whole blood cells were stained with the following monoclonal antibodies for flow cytometry analysis: anti-human CD235a-PE (clone HI264; Biolegend) and anti-mouse Ter119-PE-Cy7 (clone: TER-119; Biolegend). For overall hematopoietic engraftment, blood was collected retro-orbitally 10 to 12 weeks after engraftment. Red blood cells were lysed using ACK (Gibco) and the cells were stained with the following monoclonal antibodies for flow cytometry analysis: anti-mouse CD45-APC-Cy7(clone: 30-F11; BD Biosciences), anti-human

CD45-PE-Cy5.5(clone: HI30; Invitrogen), anti-human CD19-FITC (clone HIB19; BD Biosciences), anti-human CD3-Pacific Blue (clone S4.1; Invitrogen), anti-human NKp46-APC(clone 9E2; BD Biosciences), and anti-human CD14-PE-Cy7 (clone M5E2; Biolegend). The samples were acquired by a Fortessa (BD Biosciences) or Symphony (BD Biosciences) and analyzed using FACSDiva (BD Biosciences) and FlowJo software. Mice with ≥10% hCD45+ of total circulating CD45+ cells (total including both mouse and human CD45+ cells) were used for experiments. For experimental repeats, different donor sources of human CD34+ cells were used. Donor to donor variations in hCD45+ levels (human leukocytes) were comparable with the range of variation between individual same donor CD34+ cell engrafted mice.

Analysis of murine monocytes and macrophages

For analysis of mouse myeloid cells, single-cell suspensions were prepared from spleen and liver and mechanically digested followed by passage through a 70μM filter. RBCs were lysed using ACK (Gibco) and the cells were stained with the following monoclonal antibodies for flow cytometry analysis: anti-mouse CD45-APC-Cy7(clone: 30-F11; BD Biosciences), anti-human CD45-PE-Cy5.5(clone: HI30; Invitrogen), anti-mouse CD11b-BV605 (clone M1/70; Biolegend), anti-mouse CD14-FITC (clone: rmC5-3; BD Biosciences), anti-mouse VCAM-PE (clone: 429; BD Biosciences, anti-mouse F4/80-PE-Dazzle (clone BM8; Biolegend), anti-human CD14-PE-Cy7 (clone M5E2; Biolegend), anti-human CD206 BV785 (clone 15-2; Biolegend), and anti-human CD36 Alexa700 (clone 5-271; Biolegend). The samples were acquired by a Fortessa (BD Biosciences) or Symphony (BD Biosciences) and analyzed using FACSDiva (BD Biosciences) and FlowJo software.

hEPO treatment

Human HSC-engrafted HMOX-1$^{-/-}$ hSIRPα/hM-CSF/hCD47/Rag2$^{-/-}$/IL-2R$\gamma^{-/-}$ mice were retro-orbitally bled to analyze pre-injection levels of hRBCs and then injected with 100units of hEPO (R&D systems) intra-peritoneally. One week later, mice were again retro-orbitally bled to check hRBC and total RBC levels.

Serum chemistry and heme analysis

Blood was acquired from mice via cardiac puncture and serum and collected using serum separator tubes. Serum was used for analysis of liver enzymes including aspartate aminotransferase (AST), alanine transaminase (ALT), and alkaline phosphatase (ALP) as well as creatinine which is an indicator of kidney function. AST, ALT, ALP, and creatinine were analyzed using the ADVIA® Chemistry XPT System (Siemens).

Total human IgM and IgG were analyzed from serum through a standard sandwhich ELISA. Briefly, 96-well clear-bottom slides (Nunc) were coated with anti-human IgM or anti-human IgG capture antibodies (Jackson Immunoresearch). Plate was then blocked with PBS-Tween 20 and 5% bovine serum albumin (BSA) and diluted serum samples (HIS and normal human serum) added along with human IgM and IgG standards (Jackson Immunoresearch). Plates were washed with PBS-Tween 20 and anti-human IgM and IgG detection antibodies added that are conjugated to horse-radish peroxidase (HRP). Plate was incubated as such and then washed followed by addition of Opt EIA TMB substrate (Invitrogen) for development. Reaction was

stopped with 1N sulfuric acid and IgM and IgG levels visualized using an ELISA reader (Molecular Devices).

Serum was also analyzed for heme levels. Spleen heme levels were analyzed by mechanical digestion of spleens in PBS followed by passage through 70μM filter. Single cell suspension was centrifuged at >500g for 5mins and supernatant collected for heme analysis. Heme levels from serum and splenic supernatant was analyzed using a Heme Assay Kit (MilliporeSigma) according to manufacturer instructions. Splenic heme levels were normalized to spleen size and spleens showed no morphological differences other than size.

Tissue analysis

Liver and kidney were harvested from WT, non-engrafted HMOX-$1^{+/+}$, non-engrafted HMOX-$1^{-/-}$, engrafted HMOX-$1^{+/+}$, and engrafted HMOX-$1^{-/-}$. Tissues were fixed in 10% formalin for 24 hours and then transferred into 70% EtOH for 48 hours. The tissues were processed in the Leica Tissue Processor and paraffin embedded. 5μM sections were baked onto slides and slides were deparaffinized and rehydrated for staining. Kidney sections were stained with a Masson's Trichrome kit (Statlab) according to manufacturer's protocol. Liver and kidney sections were stained with a Prussian Blue kit (Polysciences, Inc) according to manufacturer's protocol. Liver sections were stained in Mayers Hematoxylin for 1 minute and washed with tap water. The nuclei were blued in 1XPBS for 1 minute and washed three times in distilled water. The sections were counterstained in Alcoholic-Eosin for 1 minute and then dehydrated. The slides were cleared in xylene and coversliped. Scanned whole slide images (WSI) of slides were evaluated by board-certified veterinary pathologists. Fibrosis was scored on Masson's trichome stained

sections using a semi-quantitative grading scale: 0-normal limits; 1-minimal; 2-mild; 3-moderate; 4-severe. Iron accumulation was scored on Prussian blue stained sections using a semi-quantitative grading scale: 0-normal limits; 1-Rare (<1% stained cells) 2-minimal (1-10% stained cells); 3-mild (10-30% stained cells); 4-moderate (30-60% stained cells); 5-severe (60-100% stained cells).

Single-cell RNAseq analysis

Mouse and human CD45+ cell fractions were collected from the spleens of human HSC-engrafted HMOX-$1^{+/+}$ and HMOX-$1^{-/-}$ hSIRPα/hM-CSF/hCD47/$Rag2^{-/-}$/IL-2R$\gamma^{-/-}$ mice. Cells were isolated by positive magnetic enrichment using either mouse CD45 or human CD45 microbeads (Miltenyi). Isolated cells were processed using 10x 5prime NextGEM v2 library kit. After the processing, CellRanger (v.6.1.1, 10X Genomics) with GRCh38 reference was performed on the processed cells to compute gene expression levels and to generate analysis-ready data. We checked the quality of the data (Number of cells, mean reads per cell, median genes per cell, median UMI counts per cell, etc.) to filter out artifacts, empty droplets, and multiplets. In each sample, cells with the total number of molecules detected within a cell higher than 30,000 and lower than 1,000 were filtered out. Then Python module Scanpy (v1.7.1) was used to normalize the data. The normalization was done as following: 1. Transformation of total counts so each cell sums to 10,000. 2. Log1p of the transformed counts. 3.Unit Scaling of the gene expression counts across all cells to ensure a mean of zero and a max value of 10. Lastly, R Seurat package (v4.3.0.1) was utilized to generate UMAP plots and to run clustering. In each cluster, we identified markers based on differentially expressed genes, and cell types were given to the

clusters based on the top markers. Cell type percentages were calculated by [the number of cells for the cell type x 100 / the total number of cells in the condition].

Statistical analysis

Statistical analysis was performed using Graphpad Prism (version 9.4.1; Graphad Software, San Diego, CA). Statistical significance was evaluated in most figures by unpaired student t-test. Statistical significance of hEPO treatment (Figure 4) was evaluated by paired student t-test.

Results

A 7kb mouse genomic sequence of Hmox1 gene from the start codon ATG to the stop codon was deleted on mouse chromosome 8 C1, between coordinates chr8: 75093750-75100019 (GRCm38 assembly) to make the targeting vector, which was electroporated into mouse embryonic stem (ES) cells with humanized SIRPα, humanized M-CSF, humanized CD47 and Rag2-/- IL-2Rγ-/- (Figure 1). F0 mice were bred to homozygosity for all alleles.

HMOX-1$^{-/-}$ and HMOX-1$^{+/+}$ in the (hSIRPα/hM-CSF/hCD47/Rag2$^{-/-}$/IL-2Rγ$^{-/-}$ background mice were injected intra-peritoneally with hRBCs. At day 1 post-injection, no hRBCs could detected in the peripheral blood of HMOX-1$^{+/+}$ mice (Figure 2A). In contrast, injected hRBCs survive for more than 1 week in the peripheral blood of HMOX-1$^{-/-}$ (Figure 2A). Notably, the level of total RBCs (mouse and human) was not different between HMOX-1$^{-/-}$ and HMOX-1$^{+/+}$ mice (Figure 2B).

HMOX-1$^{-/-}$ and HMOX-1$^{+/+}$ mice were engrafted with human HSCs and development of a human immune system was analyzed in these mice. After 12 weeks of engraftment, human CD45+ levels were slightly higher in HMOX-1$^{-/-}$ mice, though BM engraftment was comparable between HMOX-1$^{+/+}$ and HMOX-1$^{-/-}$ HIS mice (Figure 3A). Notably though, it has been described that down-regulation of HMOX-1 increases engraftment with murine HSCs[31]. Since HIS mice were engrafted with only 100,000 HSCs, the frequency of HSPCs in the BM is

generally too low for appreciable quantification. Nonetheless, the level of HIS engraftment is substantial. With HIS engraftment, total RBCs are significantly reduced (p<0.0001) in both HMOX-1$^{+/+}$ and HMOX-1$^{-/-}$ HIS mice (Figure 3B). This has previously been described in HIS models with humanized M-CSF due to the increased human macrophages phagocytosing murine RBCs[2]. HMOX-1$^{-/-}$ HIS mice have lower human B cells and greater human myeloid cells in blood and BM relative to HMOX-1$^{+/+}$ HIS mice (Figure 3C, D). HMOX-1$^{-/-}$ HIS mice have greater human NK cells in the BM relative to HMOX-1$^{+/+}$ HIS mice (Figure 3D). Despite lower human B cell levels in HMOX-1$^{-/-}$ HIS mice, there is significantly higher human IgG in the serum of HSC-engrafted HMOX-1$^{-/-}$ mice than in HMOX-1$^{+/+}$ HIS mice, and similar levels of serum human IgM (Supplemental Figure 1). Though both HMOX-1$^{-/-}$ and HMOX-1$^{+/+}$ HIS mice have less IgM/IgG than normal human serum (Supplemental Figure 1), common to HIS mice due to dysfunctional human B cell responses[3].

In contrast to HSC donor-matched HMOX-1$^{+/+}$ mice, human HSC-engrafted HMOX-1$^{-/-}$ mice had hRBCs in peripheral blood (Figure 3E). In the BM, both human HSC-engrafted HMOX-1$^{+/+}$ and HMOX-1$^{-/-}$ mice had hRBCs, albeit with higher levels in HMOX-1$^{-/-}$ HIS mice (Figure 3F), indicating that although hRBCs can develop in the BM of HIS mice, HMOX-1$^{-/-}$ HIS mice allow hRBCs to survive in the peripheral blood.

Erythropoietin (EPO) increases RBC output from the BM[32,33]. Injection of human EPO into human HSC-engrafted HMOX-1$^{-/-}$ mice increased the percentage (Figure 4A) and number (Figure 4B) of hRBCs in the peripheral blood. However, there was no effect on total RBC numbers (Figure 4C) since the majority of RBCs in the HMOX-1$^{-/-}$ HIS mice are murine, and hEPO does not cross-react with murine EpoR[34].

We analyzed macrophage levels in spleen and liver of HMOX-1$^{-/-}$ and HMOX-1$^{+/+}$ controls. No significant differences are noted in mouse CD11b+/CD14+ monocytes between HMOX-1$^{-/-}$ and HMOX-1$^{+/+}$ spleen, but HMOX-1$^{-/-}$ have a reduction in F4/80+/VCAM+ macrophage subset relative to HMOX-1$^{+/+}$ spleen (Figure 5A). The liver is considered a major site of hRBC clearance in mice[13]. Accordingly, we observed a reduction of murine F4/80+ macrophages in the liver of HMOX-1$^{-/-}$ relative to HMOX-1$^{+/+}$, whereas there was a concomitant increase in overall murine CD11b+ monocytes in HMOX-1$^{-/-}$ mice (Figure 5B). As observed in Figure 3B, there is an increase in human myeloid cells in the blood of HMOX-1$^{-/-}$ HIS mice, there also appears to be a slight increase in human monocytes (denoted as hCD14+) in spleen and liver of HMOX-1$^{-/-}$ HIS mice (Figure 5C). Furthermore, analysis of hCD36+/CD206+ human macrophage populations indicated an increase in this specific human macrophage population in the spleen (Figure 5C). This population is also increased in the liver of HMOX-1$^{-/-}$ HIS mice (Figure 5C).

Flow cytometric analysis has already shown a reduction in murine macrophages without a loss of overall murine monocytes in HMOX-1$^{-/-}$ mice (Figure 5). We further wanted to determine if there are differences in human leukocytes that develop from hHSC engraftment of HMOX-1$^{+/+}$ versus HMOX-1$^{-/-}$ HIS mice. Thus, single-cell RNAseq was performed on mouse and human CD45+ leukocytes isolated from the spleen of HMOX-1$^{+/+}$ and HMOX-1$^{-/-}$ mice. We first show the various subsets of murine CD45+ leukocytes in the spleen of engrafted MSRG47 mice (Figure 6A). Murine macrophages are selectively diminished in the spleen of HMOX-1$^{-/-}$ mice and these macrophages are denoted “erythroblastic” macrophages (EB macrophages) because they share genes that are commonly found on erythrocytes such as *EpoR, KLF1*, and Hemoglobin-associated genes *Hbb* and *Hba*. This subset of macrophages is involved in the

formation of erythroblastic islands for RBC maturation as well as erythrophagocytosis of senescent RBCs[35-38]. Remarkably, single-cell RNAseq analysis of human CD45+ cells in the spleen indicated a loss of human EB macrophages as well as a significant reduction in human B cells (Figure 6B). Whereas human EB macrophages are reduced in the spleen of HMOX-1$^{-/-}$, there is still an increase in overall human macrophages, confirming what was previously shown by FACS analysis (Figure 5C).

Human macrophages may be ameliorating certain pathologies exhibited by HMOX-1$^{-/-}$ mice. Elevated heme levels have been described in HMOX-1 deficient mice, and whereas heme is elevated in both serum and spleen of non-engrafted HMOX-1$^{-/-}$ mice, HIS engraftment greatly reduces both serum (Supplemental Figure 2A) and spleen heme (Supplemental Figure 2B) in HMOX-1$^{-/-}$ mice. No morphological difference between spleens other than size was observed. Engrafted mice have larger spleens due to more immune cells. Furthermore, iron deposition in the kidney of HMOX-1$^{-/-}$ mice is decreased upon HIS engraftment (Supplemental Figure 3A). No iron accumulation was observed in other groups. Minimal fibrosis was observed in interstitium among all groups (Supplemental Figure 3B). In contrast, the liver of engrafted HMOX-1$^{-/-}$ mice exhibited the highest amount of iron accumulation in the hepatocytes and Kupffer cells, followed by engrafted HMOX-1$^{+/+}$ mice (Supplemental Figure 3C). No or rare iron accumulation was observed in other groups. There was no evidence of fibrosis within the examined sections (Supplemental Figure 3D).

Liver enzymes including AST, and ALT are similar between HMOX-1$^{+/+}$ and HMOX-1$^{-/-}$ mice, whether engrafted or non-engrafted (Supplemental Figure 4A). Engraftment leads to an increase in ALP, but there is no significant difference between HMOX-1$^{+/+}$ and HMOX-1$^{-/-}$ HIS mice (Supplemental Figure 4A). Furthermore, creatinine, an indicator kidney pathology, is

normal in both HMOX-1$^{+/+}$ and HMOX-1$^{-/-}$ mice (engrafted and non-engrafted) (Supplemental Figure 4B), further supporting histology data on the lack of kidney pathology (Supplemental Figure 3B).

Discussion

We showed here that HMOX-1 deficiency in a humanized M-CSF/SIRPα/CD47 and Rag2$^{-/-}$/IL-2R$_\gamma^{-/-}$ background allows for presence of peripheral blood hRBCs, generated from hHSC engraftment or injection of hRBCs into non-engrafted mice. The survival of hRBCs in mice is dependent on removal of specific murine macrophage subsets. Unlike other approaches that utilize clodronate liposomes to remove phagocytic macrophages, HMOX-1 deletion is a genetic approach that renders the mouse environment permissive to hRBCs and does not require further manipulations. Additionally, unlike genetic deletions that ablate all murine myeloid cells, which have deleterious effects on mouse development[19], HMOX-1 deletion leads to the loss of specific murine macrophage subsets that are most associated with erythrophagocytosis as revealed by single-cell RNAseq analysis. This leads to a HIS model that permits study of hRBCs in mice.

Recently, Song et al. used a genetic approach to delete out the fumarylacetoacetate hydrolase (FAH) in the immunodeficient MISTRG mice[13]. The FAH deletion in human HSC engrafted MISTRG mice allows for ablation of murine liver cells and replacement with human liver cells[13]. Song et al. demonstrated that hRBCs in these mice are cleared in the liver by murine Kupffer cells, a tissue-specific macrophage subset, and by ablating murine liver cells there is a

decrease in murine Kupffer cells that allows for hRBC survival[13]. Despite the MISTRG-FAH model being a breakthrough for hRBCs in HIS mice, this also requires further manipulation. Murine hepatocytes are eliminated and concurrently replaced with human hepatocytes, but this requires 1) surgical implantation of human hepatocytes, and 2) at least 4 weeks of cycling the mice on/off NTBC water to achieve replacement with human liver[13,17]. With HMOX-1 deficiency in an immune-deficient mouse model, additional manipulation is unnecessary for hRBCs due to the genetic deletion of HMOX-1 eliciting a steady-state loss of specific murine macrophages. As demonstrated, hRBCs survive longer in the peripheral blood upon passive transfusion of human blood or can develop via erythropoiesis from human HSC engraftment.

Song et al. speculated that the humanized M-CSF in the MISTRG-FAH model further diminishes re-establishment of murine Kupffer cells in the murine liver upon liver humanization by skewing the balance between mouse and human myeloid cells[13]. We believe that is not occurring in our HMOX-1$^{-/-}$ HIS model because the ablation of murine macrophages occurs at steady-state without any further intervention. Furthermore, loss of murine macrophages in this model is not dependent on human HSC engraftment.

HMOX-1$^{-/-}$ in the HIS mice that we report here includes humanization of the M-CSF cytokine which increases human myeloid/macrophage levels upon human HSC-engraftment, similarly how it has been reported in the MISTRG HIS model[2,13,39]. Because of the increased human macrophages, HIS models with humanized M-CSF have a high attrition rate, primarily believed to be due to anemia resulting from the murine RBCs being phagocytosed by human macrophages[2]. Even though there are appreciable hRBCs in the peripheral blood of HMOX-1$^{-/-}$ hSIRPα/hM-CSF/hCD47/Rag2$^{-/-}$/IL-2Rγ$^{-/-}$ HIS mice, the low level of hRBCs would not be enough to overcome anemia resulting from the increased human macrophages. Thus, CD47, the

ligand for SIRPα that stimulates a "don't-eat-me-signal", is also humanized to mitigate murine RBCs being engulfed by increased human macrophages [40,41], increasing the survival of this HIS model. With the advent of a HIS model with hRBCs present in peripheral blood, the next challenge would be to increase hRBC output so to overcome this anemia resulting from humanization of M-CSF. Such a HMOX-1$^{-/-}$ HIS model with humanized M-CSF would potentially not require humanized CD47 but would rather benefit from loss of mouse RBCs and possibly a replacement with hRBCs.

HMOX-1$^{-/-}$ HIS mice have even higher levels of human myeloid cells and human CD36+/CD206+ macrophages than HMOX-1$^{+/+}$ HIS mice. In the liver, this indicates there is an increase in human Kupffer cells. One theory behind this observation is that the loss of murine macrophages opens a cellular niche that enhances human macrophage development. Increased human NK cells are also observed in certain tissues which is probably a result of elevated human myeloid cells that produce human IL-15, potentiating human NK cell development[2,4].

Despite an overall increase in human macrophages, single-cell RNAseq analysis of the human immune compartment in HSC-engrafted HMOX-1$^{-/-}$ mice revealed that there is also a loss of specific human macrophages subsets that have a similar genetic signature (denoted by *EpoR* and *HMOX-1* genes) as the murine macrophage population lost in HMOX-1$^{-/-}$ mice. Upon loss of murine erythrophagocytic cells, there is a subsequent dysregulation of the iron recycling pathway with oxidatively-stressed RBCs that have an increased lifespan to compensate for the anemia resulting from this dysregulation[27,42]. However, it is possible that specific human erythrophagocytic macrophage subsets are engulfing oxidatively-stressed mouse RBCs and the macrophages are being overloaded with toxic heme which supplants the capacity of HMOX-1$^{+/+}$ human macrophages to deal with. Furthermore, there may secondary byproducts produced in the

blood of HMOX-1$^{-/-}$ mice (increased ferritin, bilirubin, etc.) that may have deleterious effects on phagocytic human macrophages. Additional in vitro studies with HMOX-1$^{+/+}$ vs HMOX-1$^{-/-}$ mouse blood added to human macrophages could shed light on this loss of specific human EB macrophages. Even more surprising is the reduction in human B cells in the spleen of HSC-engrafted HMOX-1$^{-/-}$ mice. Loss of mouse B cells has not been reported in immune-competent HMOX-1$^{-/-}$ mouse models. Theoretically, soluble byproducts generated in HMOX-1$^{-/-}$ blood are having a specific effect on human B cells in the peripheral tissues. Alternatively, HIS engraftment is increased in HMOX-1$^{-/-}$ mice with increased myeloid/NK cells. It is possible that skewing towards myeloid/NK cells may be impacting human B cell lymphoiesis.

There is evidence that human macrophages in the HMOX-1$^{-/-}$ HIS mice are compensating for the loss of murine erythryophagocytic macrophages due to amelioration of certain pathologies associated with HMOX-1$^{-/-}$ mice[23,26,29]. Elevated heme levels in serum and spleen, as well as iron deposition in the kidney of HMOX-1$^{-/-}$ mice are decreased upon HIS engraftment. This suggests that human macropahges may be clearing excessive heme and iron upon HIS engraftment. Similarly, Kovtunovych et al. showed that BM transfer of WT mouse BM ameliorated pathology observed in HMOX-1 deficient mice[29]. Although, non-engrafted HMOX-1$^{-/-}$ mice are comparable to non-engrafted HMOX-1$^{+/+}$ mice as noted by lack of any severe kidney/liver pathology and further shown by serum chemistry. Indeed, HMOX-1$^{-/-}$ mice in an immune-deficient background appear to be healthier than described in an immune-competent background which has been reported to have scvere kidney/liver pathology. Furthermore, due to pathologies, HMOX-1$^{-/-}$ mice have to be generated from HMOX-1$^{+/-}$ intercrosses[23], whereas HMOX-1$^{-/-}$ mice in an MSRG47 background can be bred through HMOX-1$^{-/-}$ intercrosses. A benefit of this reduction in pathology is that it renders the HMOX-1$^{-/-}$ HIS mouse model more

practical for experimental usage and preclinical testing due to ease of breeding, longer life-span, etc.

Overall, a major advantage for the HMOX-1$^{-/-}$ HIS model is the study of hematological diseases that affect hRBCs such as sickle cell anemia and beta-thalassemia[13]. Human HSCs from patients with such hematological diseases could be engrafted into HMOX-1$^{-/-}$ HIS mice providing an in vivo model to test potential therapeutics[13]. A limitation still remains that most RBCs are still murine and so hRBC output from the BM needs to be enhanced in the HMOX-1$^{-/-}$ HIS model. Such low frequency limits the ability to study hEPO function in vivo since the primary purpose of RBCs to ferry oxygen is primarily carried out by the mouse RBCs. Human erythroblast reconstitution still remains relatively too low and variable to comprehensively assess function and ontogenic development. Thus, to further potentiate the practicality of this mouse model, additional strategies are warranted to increase hRBC output since HMOX-1 deficiency allows hRBC peristence in peripheral blood. Since hEPO can increase hRBCs in the peripheral blood of engrafted mice, humanization of EPO in this mouse model may potentiate hRBC levels.

In vivo models of malaria have been impeded by the lack of hRBCs in mouse models since malaria parasites specifically infect hRBCs[17]. A HIS mouse model that also has hRBCs potentially can be utilized to test human-specific immune-modulatory therapeutics in an in vivo malaria model.

Acknowledgements

We thank Mark Eckersdorff for help in manuscript preparation. Additionally, we would like to thank Hans Gartner for cloning the HMOX-1 deletion into the MSRG47 ES cells and Melanie Buckman for help with mouse colony management.

Authorship

A.K.P. and K.T. engrafted mice and performed experiments. H.K. and W.K.L. analyzed molecular profiling data. C.A. and S.P. prepared samples for single-cell RNAseq. M.N., Y.W., and G.S.A. provided guidance on molecular profiling of mouse and human samples. P.B. performed serum chemistry analysis. V.K. and D.A. analyzed histology. J.Z. managed mouse husbandry and establishment of the MSRG47 HMOX-1$^{-/-}$ mouse line. N.T. designed the HMOX-1 deletion to be cloned and targeted. L.M. and A.M. provided support and guidance on this project. D.F. developed the idea of using HMOX-1 deficient mice for hRBC survival, led the project, and wrote the manuscript.

Competing Interests: Authors declare they have no competing interests.

Materials & Correspondence: Correspondence and material requests should be addressed to Davor Frleta.

References

1. Hu Z, Yang YG. Full reconstitution of human platelets in humanized mice after macrophage depletion. *Blood*. Aug 23 2012;120(8):1713-6. doi:10.1182/blood-2012-01-407890
2. Rongvaux A, Willinger T, Martinek J, et al. Development and function of human innate immune cells in a humanized mouse model. *Nat Biotechnol*. Apr 2014;32(4):364-72. doi:10.1038/nbt.2858
3. Yu H, Borsotti C, Schickel JN, et al. A novel humanized mouse model with significant improvement of class-switched, antigen-specific antibody production. *Blood*. Feb 23 2017;129(8):959-969. doi:10.1182/blood-2016-04-709584
4. Herndler-Brandstetter D, Shan L, Yao Y, et al. Humanized mouse model supports development, function, and tissue residency of human natural killer cells. *Proc Natl Acad Sci U S A*. Nov 7 2017;114(45):E9626-E9634. doi:10.1073/pnas.1705301114
5. Lee YS, O'Brien LJ, Walpole CM, et al. Human CD141(+) dendritic cells (cDC1) are impaired in patients with advanced melanoma but can be targeted to enhance anti-PD-1 in a humanized mouse model. *J Immunother Cancer*. Mar 2021;9(3)doi:10.1136/jitc-2020-001963
6. Ma SD, Xu X, Jones R, et al. PD-1/CTLA-4 Blockade Inhibits Epstein-Barr Virus-Induced Lymphoma Growth in a Cord Blood Humanized-Mouse Model. *PLoS Pathog*. May 2016;12(5):e1005642. doi:10.1371/journal.ppat.1005642
7. Wei J, Montalvo-Ortiz W, Yu L, et al. CD22-targeted CD28 bispecific antibody enhances antitumor efficacy of odronextamab in refractory diffuse large B cell lymphoma models. *Sci Transl Med*. Nov 9 2022;14(670):eabn1082. doi:10.1126/scitranslmed.abn1082
8. Wen J, Wang L, Ren J, et al. Nanoencapsulated rituximab mediates superior cellular immunity against metastatic B-cell lymphoma in a complement competent humanized mouse model. *J Immunother Cancer*. Feb 2021;9(2)doi:10.1136/jitc-2020-001524
9. Wong KK, Brenneman F, Chesney A, Spaner DE, Gorczynski RM. Soluble CD200 is critical to engraft chronic lymphocytic leukemia cells in immunocompromised mice. *Cancer Res*. Oct 1 2012;72(19):4931-43. doi:10.1158/0008-5472.CAN-12-1390

10. Garcia-Perez L, van Roon L, Schilham MW, Lankester AC, Pike-Overzet K, Staal FJT. Combining Mobilizing Agents with Busulfan to Reduce Chemotherapy-Based Conditioning for Hematopoietic Stem Cell Transplantation. *Cells*. Apr 30 2021;10(5)doi:10.3390/cells10051077
11. Zheng Y, Sefik E, Astle J, et al. Human neutrophil development and functionality are enabled in a humanized mouse model. *Proc Natl Acad Sci U S A*. Oct 25 2022;119(43):e2121077119. doi:10.1073/pnas.2121077119
12. Coughlan AM, Harmon C, Whelan S, et al. Myeloid Engraftment in Humanized Mice: Impact of Granulocyte-Colony Stimulating Factor Treatment and Transgenic Mouse Strain. *Stem Cells Dev*. Apr 1 2016;25(7):530-41. doi:10.1089/scd.2015.0289
13. Song Y, Shan L, Gbyli R, et al. Combined liver-cytokine humanization comes to the rescue of circulating human red blood cells. *Science*. Mar 5 2021;371(6533):1019-1025. doi:10.1126/science.abe2485
14. Little MA, Al-Ani B, Ren S, et al. Anti-proteinase 3 anti-neutrophil cytoplasm autoantibodies recapitulate systemic vasculitis in mice with a humanized immune system. *PLoS One*. 2012;7(1):e28626. doi:10.1371/journal.pone.0028626
15. Brainard DM, Seung E, Frahm N, et al. Induction of robust cellular and humoral virus-specific adaptive immune responses in human immunodeficiency virus-infected humanized BLT mice. *J Virol*. Jul 2009;83(14):7305-21. doi:10.1128/JVI.02207-08
16. Hu Z, Van Rooijen N, Yang YG. Macrophages prevent human red blood cell reconstitution in immunodeficient mice. *Blood*. Nov 24 2011;118(22):5938-46. doi:10.1182/blood-2010-11-321414
17. Foquet L, Schafer C, Minkah NK, et al. Plasmodium falciparum Liver Stage Infection and Transition to Stable Blood Stage Infection in Liver-Humanized and Blood-Humanized FRGN KO Mice Enables Testing of Blood Stage Inhibitory Antibodies (Reticulocyte-Binding Protein Homolog 5) In Vivo. *Front Immunol*. 2018;9:524. doi:10.3389/fimmu.2018.00524
18. Yamaguchi T, Katano I, Otsuka I, et al. Generation of Novel Human Red Blood Cell-Bearing Humanized Mouse Models Based on C3-Deficient NOG Mice. *Front Immunol*. 2021;12:671648. doi:10.3389/fimmu.2021.671648
19. Dai XM, Ryan GR, Hapel AJ, et al. Targeted disruption of the mouse colony-stimulating factor 1 receptor gene results in osteopetrosis, mononuclear phagocyte deficiency, increased primitive progenitor cell frequencies, and reproductive defects. *Blood*. Jan 1 2002;99(1):111-20. doi:10.1182/blood.v99.1.111
20. Gyori DS, Mocsai A. Osteoclast Signal Transduction During Bone Metastasis Formation. *Front Cell Dev Biol*. 2020;8:507. doi:10.3389/fcell.2020.00507
21. Mun SH, Park PSU, Park-Min KH. The M-CSF receptor in osteoclasts and beyond. *Exp Mol Med*. Aug 2020;52(8):1239-1254. doi:10.1038/s12276-020-0484-z
22. Keshvari S, Caruso M, Teakle N, et al. CSF1R-dependent macrophages control postnatal somatic growth and organ maturation. *PLoS Genet*. Jun 2021;17(6):e1009605. doi:10.1371/journal.pgen.1009605
23. Poss KD, Tonegawa S. Heme oxygenase 1 is required for mammalian iron reutilization. *Proc Natl Acad Sci U S A*. Sep 30 1997;94(20):10919-24. doi:10.1073/pnas.94.20.10919
24. Kawashima A, Oda Y, Yachie A, Koizumi S, Nakanishi I. Heme oxygenase-1 deficiency: the first autopsy case. *Hum Pathol*. Jan 2002;33(1):125-30. doi:10.1053/hupa.2002.30217

25. Yachie A, Niida Y, Wada T, et al. Oxidative stress causes enhanced endothelial cell injury in human heme oxygenase-1 deficiency. *J Clin Invest*. Jan 1999;103(1):129-35. doi:10.1172/JCI4165
26. Kovtunovych G, Eckhaus MA, Ghosh MC, Ollivierre-Wilson H, Rouault TA. Dysfunction of the heme recycling system in heme oxygenase 1-deficient mice: effects on macrophage viability and tissue iron distribution. *Blood*. Dec 23 2010;116(26):6054-62. doi:10.1182/blood-2010-03-272138
27. Fraser ST, Midwinter RG, Coupland LA, et al. Heme oxygenase-1 deficiency alters erythroblastic island formation, steady-state erythropoiesis and red blood cell lifespan in mice. *Haematologica*. May 2015;100(5):601-10. doi:10.3324/haematol.2014.116368
28. Poss KD, Tonegawa S. Reduced stress defense in heme oxygenase 1-deficient cells. *Proc Natl Acad Sci U S A*. Sep 30 1997;94(20):10925-30. doi:10.1073/pnas.94.20.10925
29. Kovtunovych G, Ghosh MC, Ollivierre W, et al. Wild-type macrophages reverse disease in heme oxygenase 1-deficient mice. *Blood*. Aug 28 2014;124(9):1522-30. doi:10.1182/blood-2014-02-554162
30. Kim KS, Zhang DL, Kovtunovych G, et al. Infused wild-type macrophages reside and self-renew in the liver to rescue the hemolysis and anemia of Hmox1-deficient mice. *Blood Adv*. Oct 23 2018;2(20):2732-2743. doi:10.1182/bloodadvances.2018019737
31. Adamiak M, Moore JBt, Zhao J, et al. Downregulation of Heme Oxygenase 1 (HO-1) Activity in Hematopoietic Cells Enhances Their Engraftment After Transplantation. *Cell Transplant*. 2016;25(7):1265-76. doi:10.3727/096368915X688957
32. Malik J, Kim AR, Tyre KA, Cherukuri AR, Palis J. Erythropoietin critically regulates the terminal maturation of murine and human primitive erythroblasts. *Haematologica*. Nov 2013;98(11):1778-87. doi:10.3324/haematol.2013.087361
33. Fouquet G, Thongsa-Ad U, Lefevre C, et al. Iron-loaded transferrin potentiates erythropoietin effects on erythroblast proliferation and survival: a novel role through transferrin receptors. *Exp Hematol*. Jul 2021;99:12-20 e3. doi:10.1016/j.exphem.2021.05.005
34. Manz MG. Human-hemato-lymphoid-system mice: opportunities and challenges. *Immunity*. May 2007;26(5):537-41. doi:10.1016/j.immuni.2007.05.001
35. Romano L, Seu KG, Papoin J, et al. Erythroblastic islands foster granulopoiesis in parallel to terminal erythropoiesis. *Blood*. Oct 6 2022;140(14):1621-1634. doi:10.1182/blood.2022015724
36. Li W, Wang Y, Zhao H, et al. Identification and transcriptome analysis of erythroblastic island macrophages. *Blood*. Aug 1 2019;134(5):480-491. doi:10.1182/blood.2019000430
37. Li W, Guo R, Song Y, Jiang Z. Erythroblastic Island Macrophages Shape Normal Erythropoiesis and Drive Associated Disorders in Erythroid Hematopoietic Diseases. *Front Cell Dev Biol*. 2020;8:613885. doi:10.3389/fcell.2020.613885
38. An X, Mohandas N. Erythroblastic islands, terminal erythroid differentiation and reticulocyte maturation. *Int J Hematol*. Feb 2011;93(2):139-143. doi:10.1007/s12185-011-0779-x
39. Rathinam C, Poueymirou WT, Rojas J, et al. Efficient differentiation and function of human macrophages in humanized CSF-1 mice. *Blood*. Sep 15 2011;118(11):3119-28. doi:10.1182/blood-2010-12-326926

40. Swoboda DM, Sallman DA. The promise of macrophage directed checkpoint inhibitors in myeloid malignancies. *Best Pract Res Clin Haematol*. Dec 2020;33(4):101221. doi:10.1016/j.beha.2020.101221
41. Oronsky B, Carter C, Reid T, Brinkhaus F, Knox SJ. Just eat it: A review of CD47 and SIRP-alpha antagonism. *Semin Oncol*. Apr-Jun 2020;47(2-3):117-124. doi:10.1053/j.seminoncol.2020.05.009
42. Cao YA, Kusy S, Luong R, Wong RJ, Stevenson DK, Contag CH. Heme oxygenase-1 deletion affects stress erythropoiesis. *PLoS One*. 2011;6(5):e20634. doi:10.1371/journal.pone.0020634

Figure legends

Figure 1: HMOX-1 KO design

A 7kb mouse genomic sequence of the mouse Hmox-1 gene, from the start codon ATG to the stop codon, was deleted on mouse chromosome 8 C1, between coordinates chr8: 75093750-75100019. The deletion was performed in ES cells with humanized M-CSF, SIRPa, CD47 and deletion of mouse Rag2 and IL-2Rγ genes. The mouse embryo comprising the donor ES cells was incubated *in vitro* and then implanted into a surrogate mother to produce an F0 mouse fully derived from the donor ES cells. Mice with Hmox-1 gene deleted were identified by genotyping using the MOA assay described above. Mice heterozygous for deletion of Hmox-1 gene were bred to homozygosity for all genes**.**

Figure 2: Injected hRBCs survive longer in HMOX-1$^{-/-}$ mice relative to HMOX-1$^{+/+}$ mice

Human RBCs were injected intra-peritoneally into non- engrafted HMOX-1$^{+/+}$ (n=7) and HMOX-1$^{-/-}$ MSRG47 mice (n=7). Mice were bled retro-orbitally at days 1, 2, 6, and 8 post-injection and

analyzed for human RBCs (hCD235a+) vs mouse RBCs (Ter-119+). **A**) Number of hRBCs per μL of blood. **B**) Total RBCs (human and mouse**)** per μL of blood.

Figure 3: HMOX-1$^{-/-}$ HIS mice have hRBCs in peripheral blood

HMOX-1$^{-/-}$ and HMOX-1$^{+/+}$ MSRG47 were intra-hepatically engrafted with human HSCs and 12 weeks post-engraftment mice were examined for **A**) total circulating hCD45+ cells (human leukocytes) in the peripheral blood and BM. **B**) Total RBC levels in the blood of non-engrafted vs engrafted HMOX-1$^{+/+}$ and HMOX-1$^{-/-}$ mice. **C**) Levels of human CD3+ T cells, CD19+ B cells, NKp46+ NK cells, and CD14+ myeloid cells (as percentage of total hCD45+ cells) are shown in the blood. **D**) Levels of human CD3+ T cells, CD19+ B cells, NKp46+ NK cells, and CD14+ myeloid cells (as percentage of total hCD45+ cells) are shown in the BM. HMOX-1$^{+/+}$ compared to HMOX-1$^{-/-}$: T cells-no significant difference, blood B cells-*p*=0.006, BM B cells-*p*=0.0005, blood NK cells-no significant difference, BM NK cells-*p*=0.0059, blood myeloid cells-*p*=0.03, and BM myeloid cells- *p*=0.01. **E**) Number of human RBCs per μL of blood of HMOX-1$^{+/+}$ and HSC donor-matched HMOX-1$^{-/-}$ HIS mice. At least 7 independent experiments were performed. **F**) Total number of hRBCs in the BM of HMOX-1$^{+/+}$ and HSC donor-matched HMOX-1$^{-/-}$ HIS mice is shown. Data represents the mean ± SEM with individual mice shown. Statistical analysis was evaluated by unpaired student t-test. Experimental analysis was performed at least 3x with representative analysis shown.

Figure 4: Human EPO increases hRBC levels in peripheral blood of HMOX-1$^{-/-}$ HIS mice

HMOX-1$^{-/-}$ MSRG47 were intra-hepatically engrafted with human HSCs and 12 weeks post-engraftment mice bled retro-orbitally to examine level of hRBCs in peripheral blood before being injected intra-peritoneally with 100 Units of human EPO. One week post-injection, hRBCs were again re-assessed from retro-orbital bleed. **A**) Percent of hRBCs in peripheral blood of HMOX-1$^{-/-}$ MSRG47 mice pre- and post-hEPO treatment. **B**) Total # of hRBCs per μL of peripheral blood pre- and post-hEPO treatment. **C**) Total # of RBCs per μL of peripheral blood pre- and post-hEPO treatment. Two independent experiments were performed. Data represents the mean ± SEM with individual mice shown. Statistical analysis was evaluated by paired student t-test.

Figure 5: HMOX-1$^{-/-}$ HIS mice have reduced murine macrophages but no decrease in monocytes

HMOX-1$^{-/-}$ and HMOX-1$^{+/+}$ MSRG47 mice were hHSC-engrafted and 12 weeks post-engraftment, spleen and liver was harvested for single-cell preparation. Mouse monocytes and macrophages were analyzed in spleen by examining mouse CD45+ leukocytes for CD11b+/CD14+ (monocytes) with macrophages denoted as mouse VCAM+/mouse F4/80+ cells (**A**). **B**) For liver analysis, mouse CD45+ leukocytes were analyzed for CD11b+ cells (monocytes) and macrophages denoted as a subset of CD11b+ cells that are mouse VCAM+/mouse F4/80+. **C**) Human monocytes and macrophages were analyzed in spleen and liver by examining human CD45+ leukocytes for CD14+ (monocytes) with CD36+/CD206+ macrophages examined as a sub-population of human CD14+ cells in spleen and liver. At least 3 independent experiments were performed. Data represents the mean ± SEM with individual mice shown. Statistical analysis was evaluated by unpaired student t-test.

Figure 6: Single-cell RNAseq analysis reveals loss of splenic mouse and human erythroblastic macrophages in HMOX-1$^{-/-}$ HIS mice

Mouse and human CD45+ cells were purified by positive magnetic isolation from hHSC-engrafted HMOX-1$^{-/-}$ and HMOX-1$^{+/+}$ MSRG47 mice. Mouse and human CD45+ cells were individually analyzed by single-cell RNAseq and UMAPs shown for mouse CD45+ cells (**A**) and human CD45+ cells (**B**). Tables to the right of the UMAPs show changes in specific leukocyte subsets between HMOX-1$^{-/-}$ (KO) and HMOX-1$^{+/+}$ (WT).

Figure 1: HMOX-1 KO design

(hM-CSF/hSIRPα/hCD47/Rag2$^{-/-}$/IL-2R$\gamma^{-/-}$ ES cell)

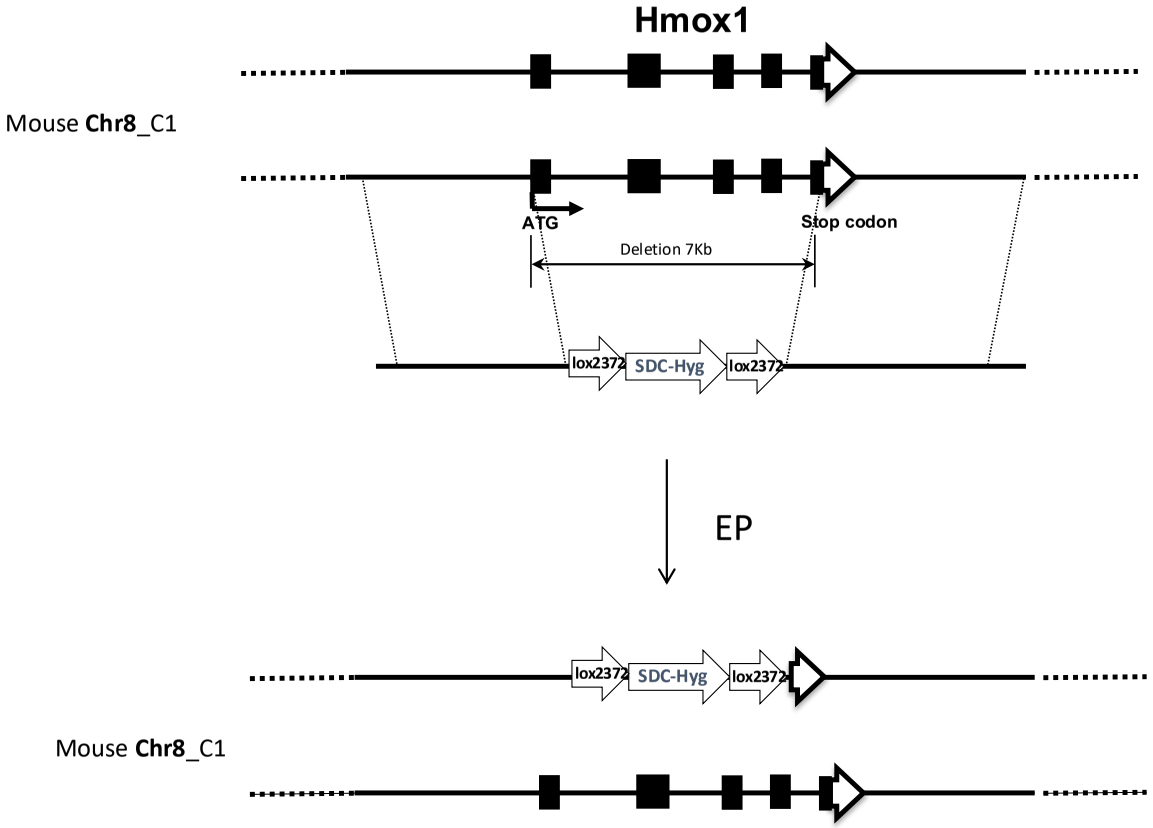

Figure 2

Figure 2: Injected hRBCs survive longer in HMOX-1$^{-/-}$ mice relative to HMOX-1$^{+/+}$ mice

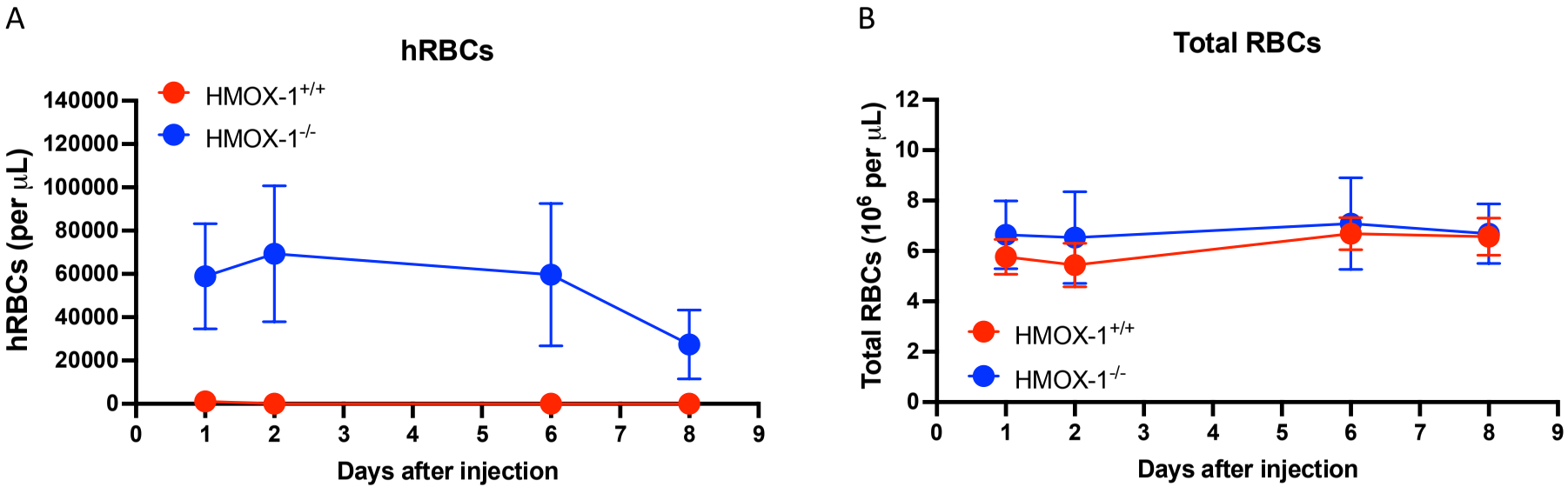

Figure 3

Figure 3: HMOX-1$^{-/-}$ HIS mice have hRBCs in peripheral blood

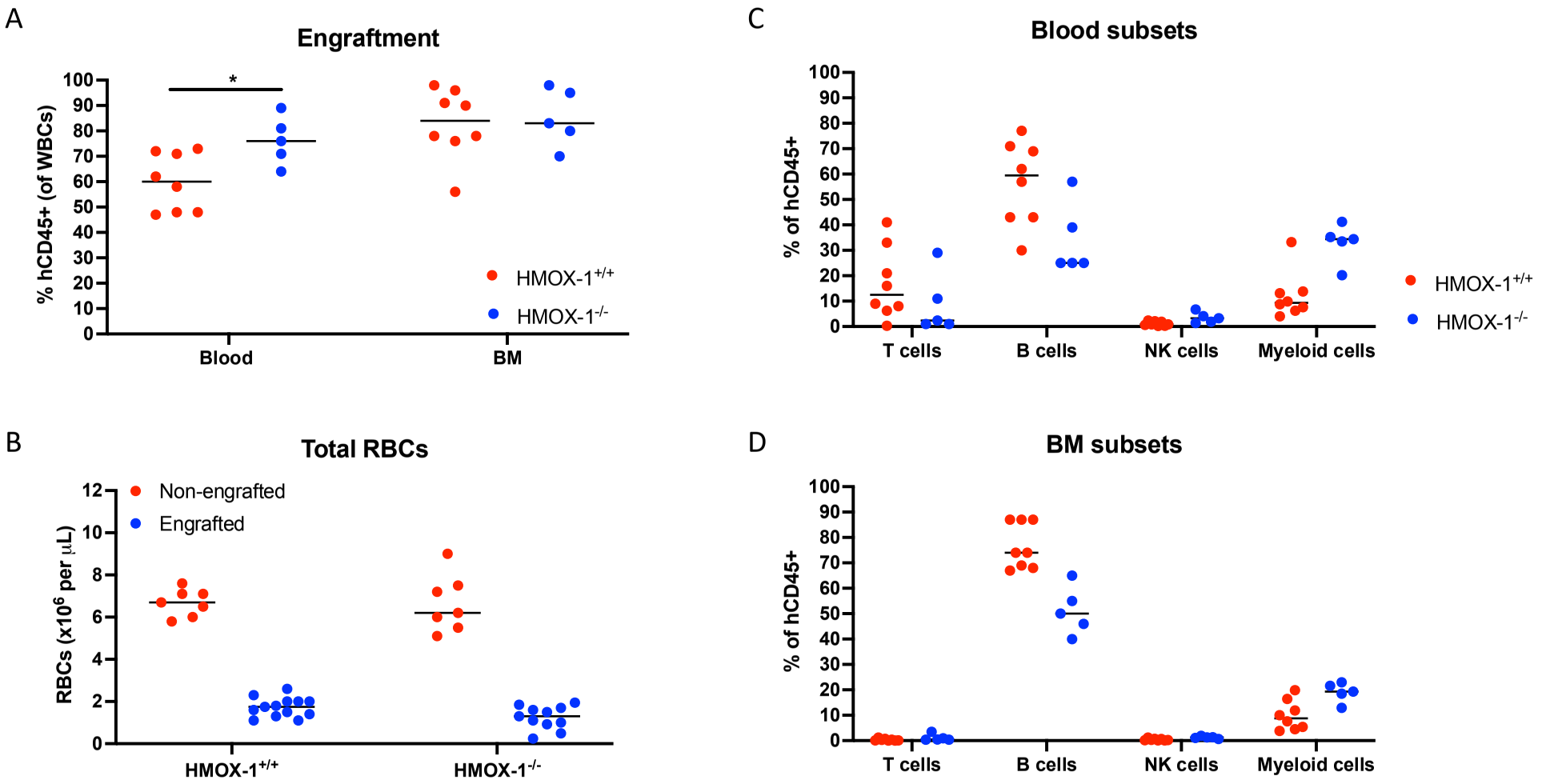

Figure 3: HMOX-1$^{-/-}$ HIS mice have hRBCs in peripheral blood

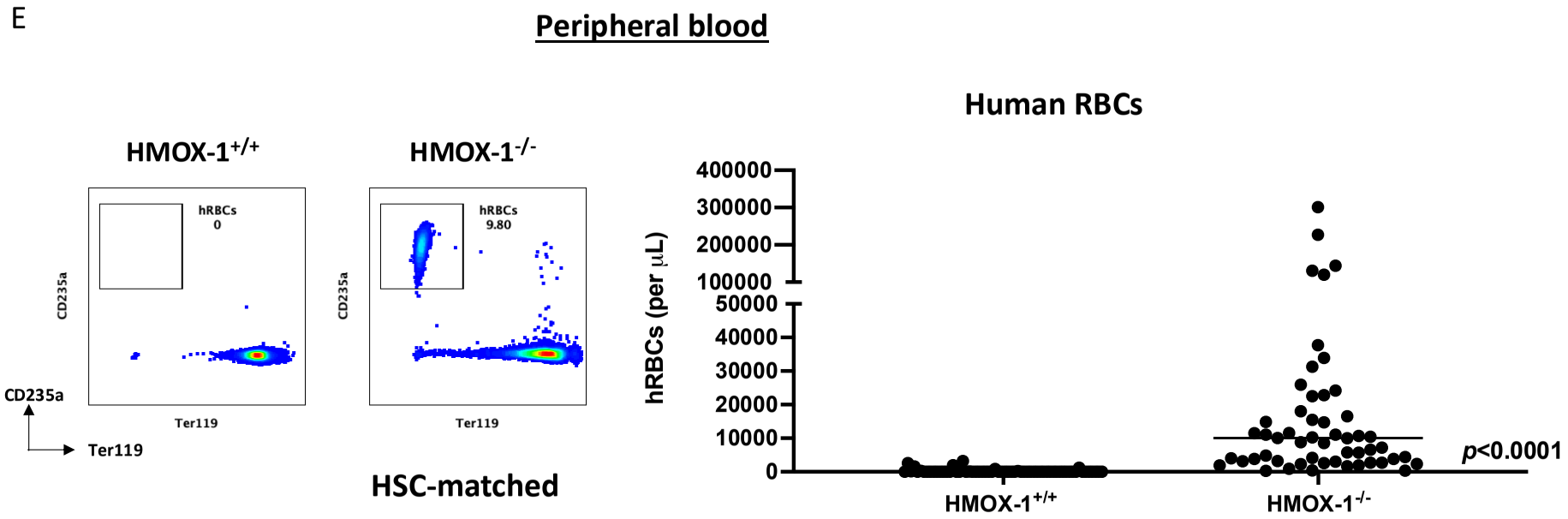

Figure 3: HMOX-1$^{-/-}$ HIS mice have hRBCs in peripheral blood

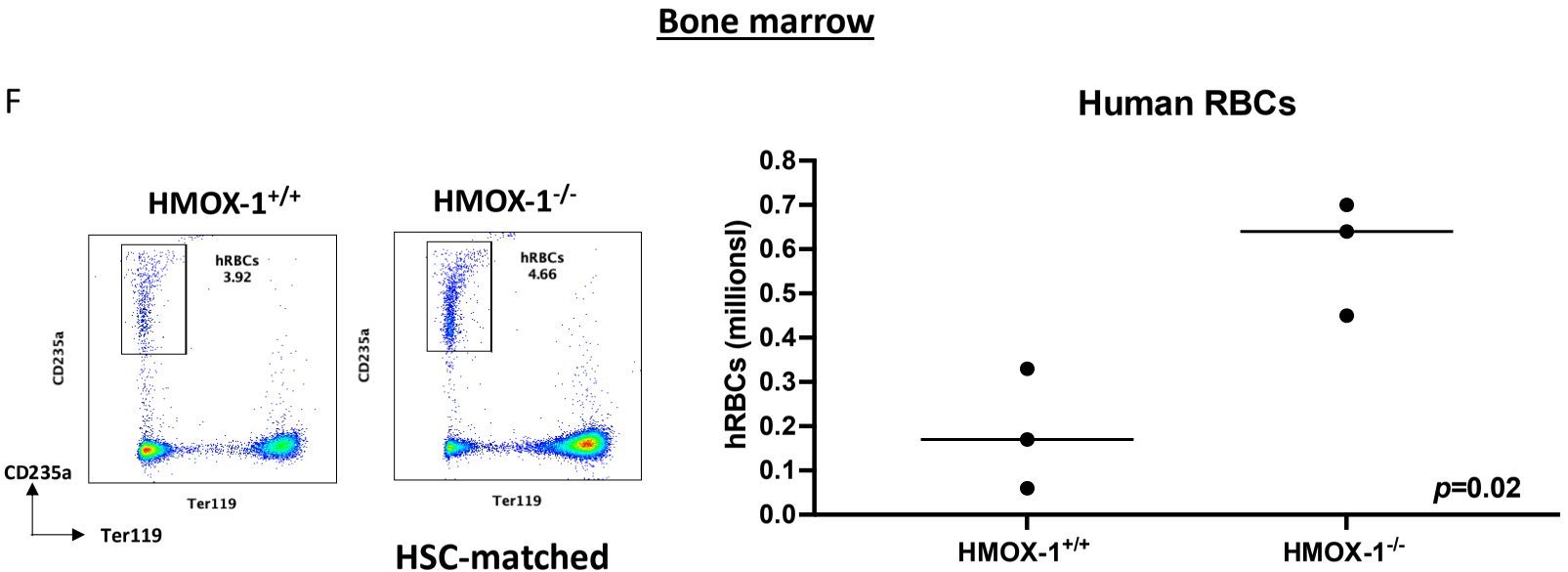

Figure 4: Human EPO increases hRBC levels in peripheral blood of HMOX-1$^{-/-}$ HIS mice

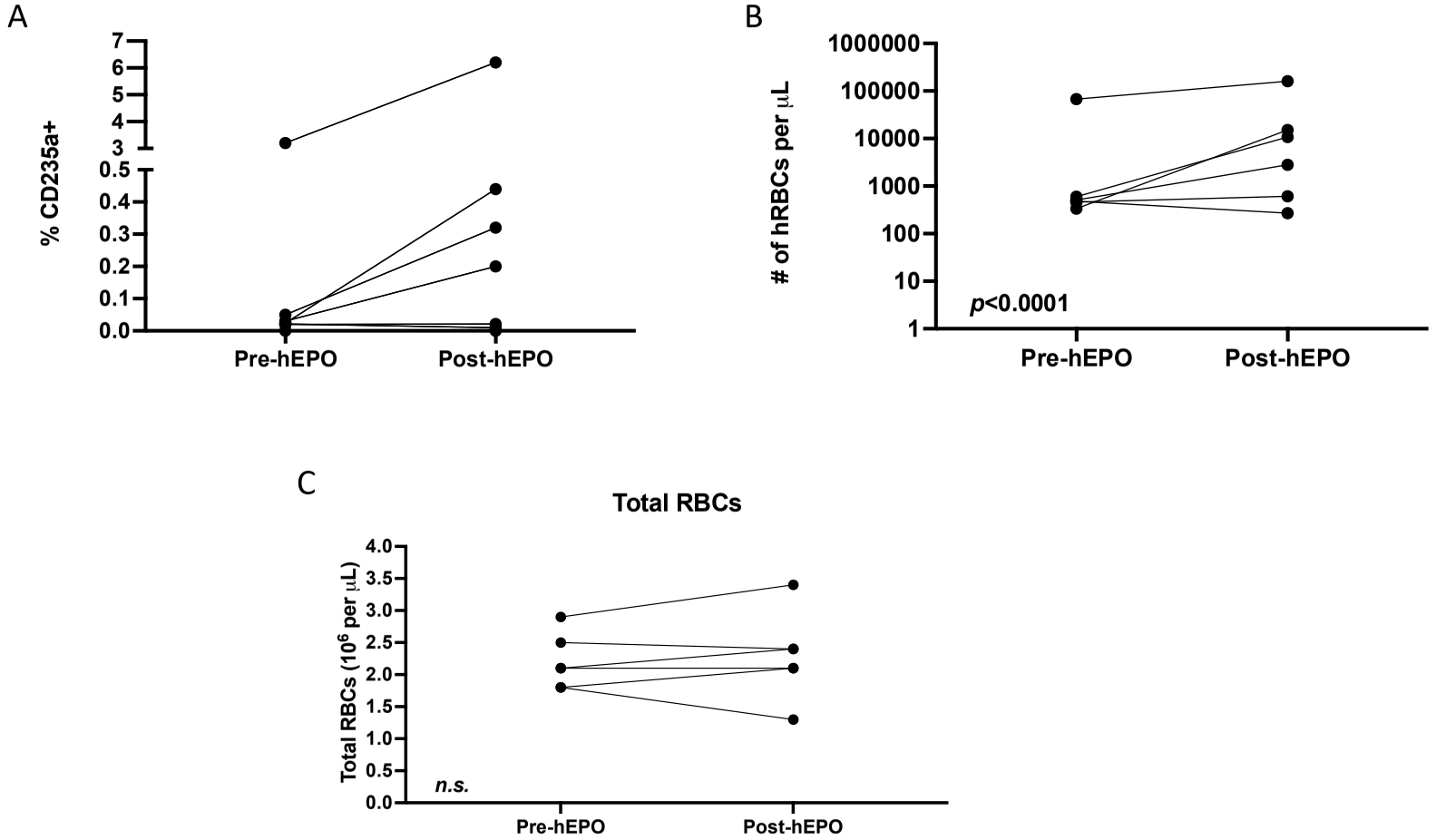

Figure 5

Figure 5: HMOX-1$^{-/-}$ HIS mice have reduced mouse macrophages but no decrease in monocytes

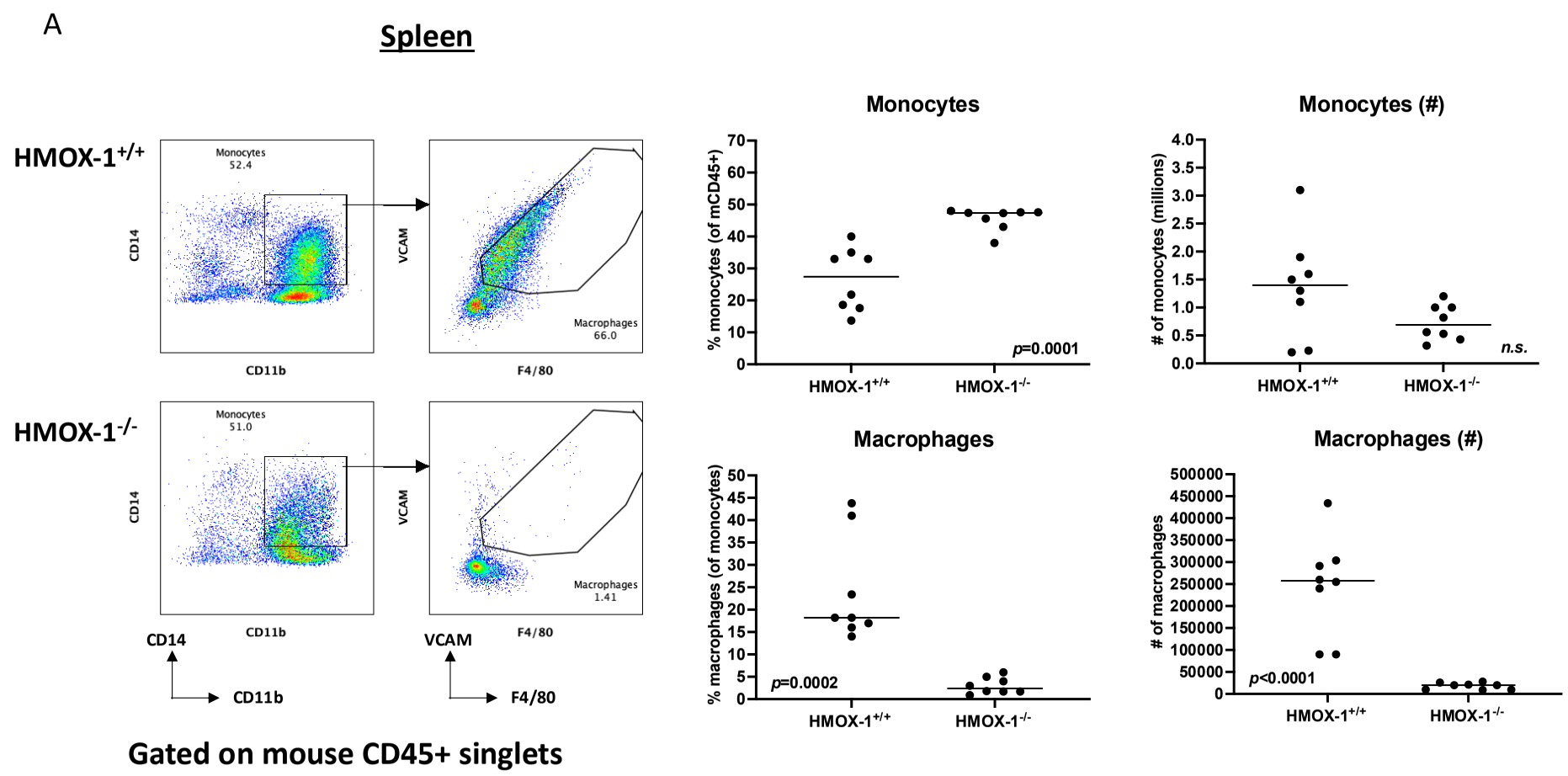

Figure 5

Figure 5: HMOX-1$^{-/-}$ HIS mice have reduced mouse macrophages but no decrease in monocytes

B

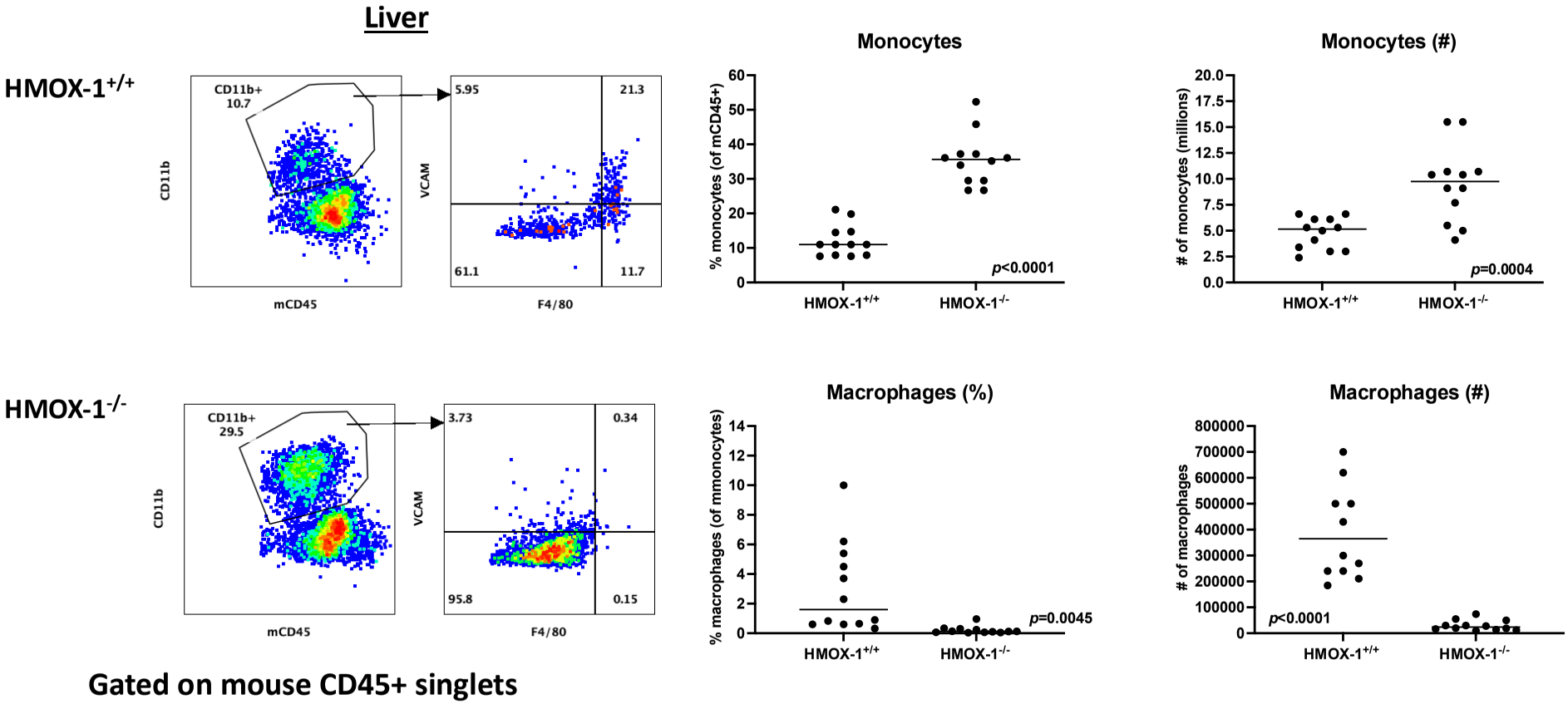

Figure 5

Figure 5: HMOX-1$^{-/-}$ HIS mice have reduced mouse macrophages but no decrease in monocytes

C

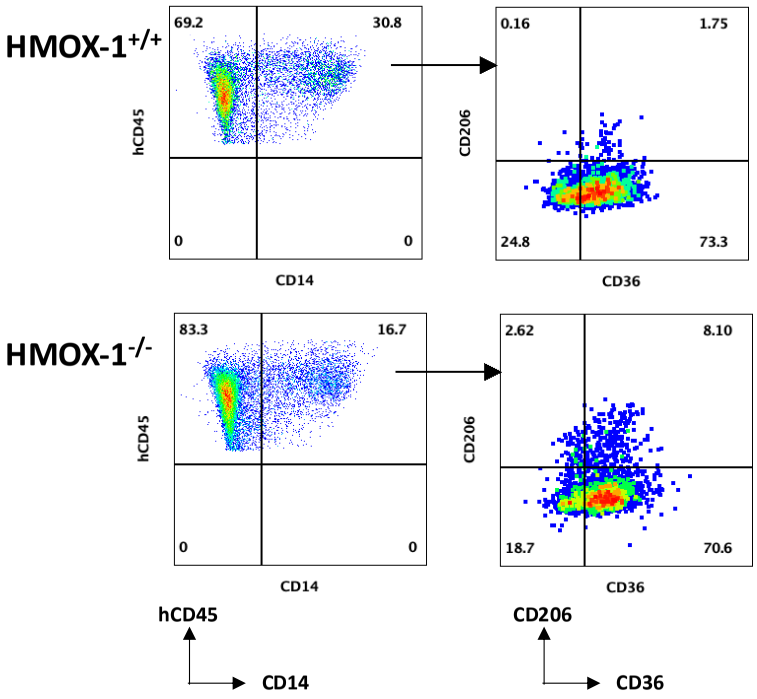

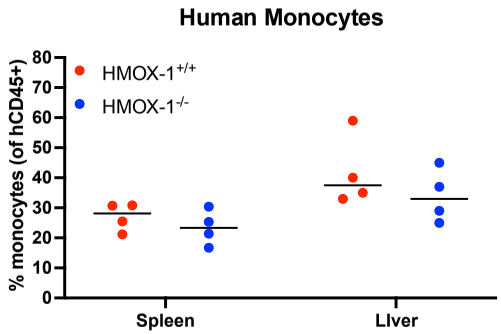

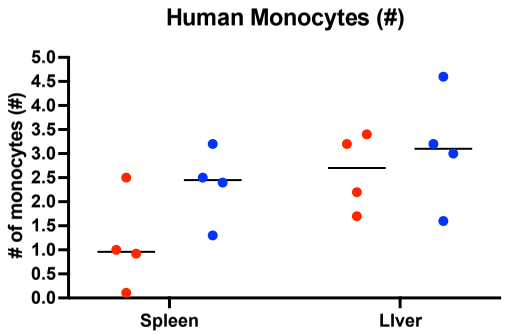

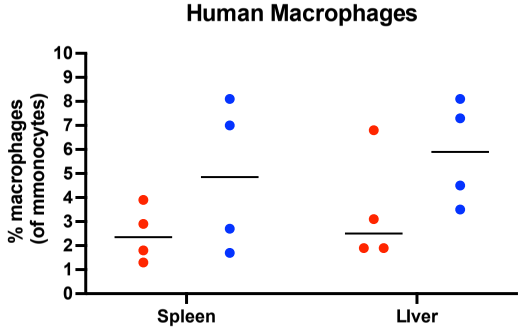

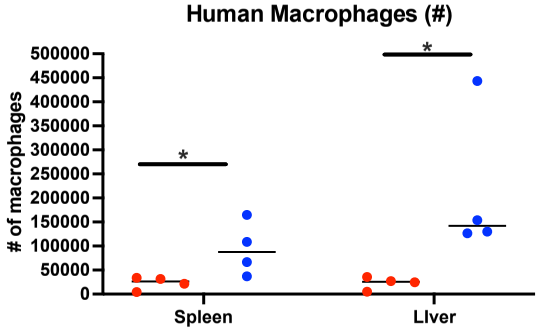

Gated on human CD45+ singlets

Figure 6

Figure 6: Single-cell RNAseq analysis reveals loss of splenic mouse and human erythroblastic macrophages in HMOX-1$^{-/-}$ HIS mice

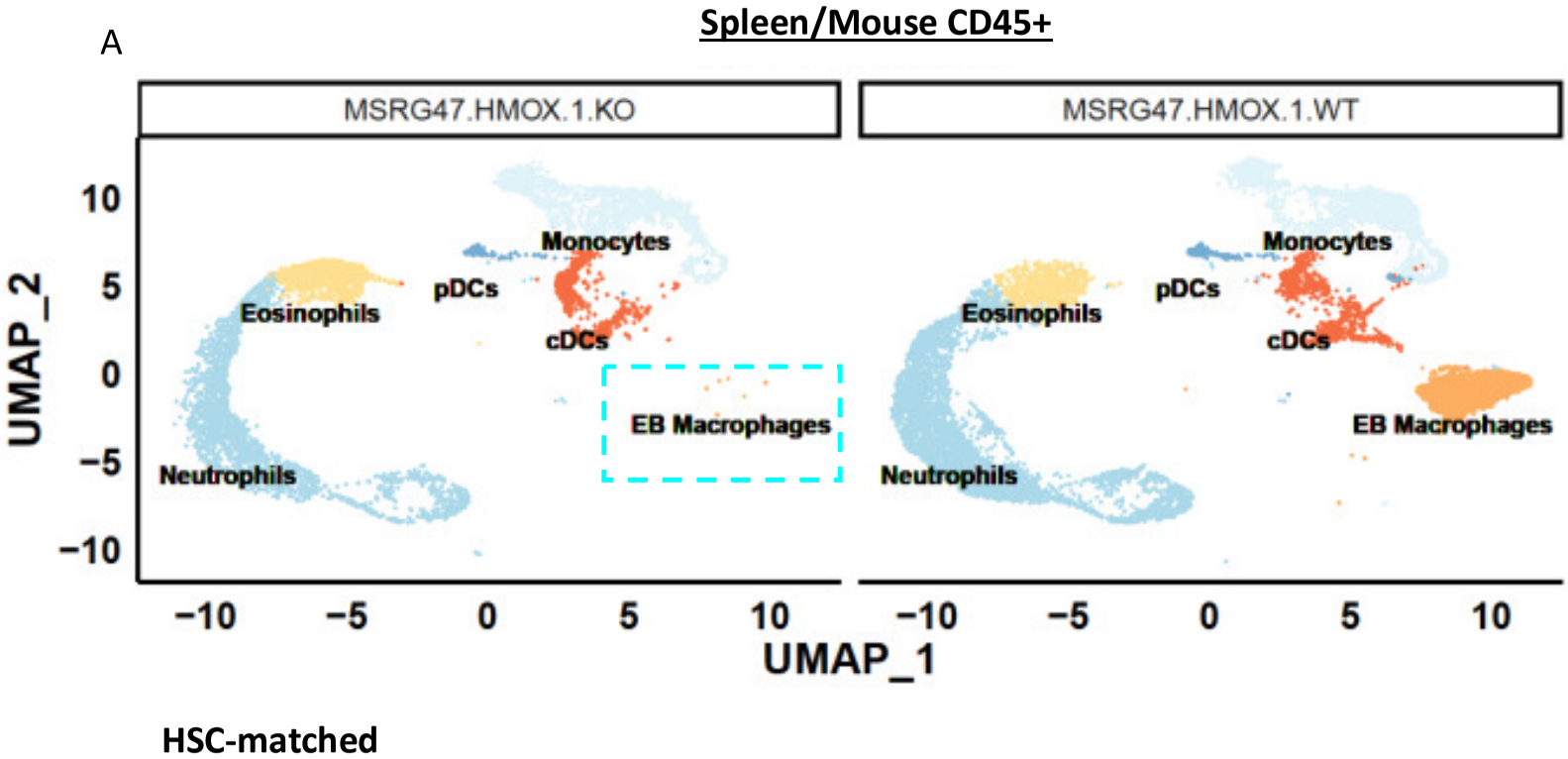

Cell %	KO	WT
EB Macrophages	0.103	20.7
Monocytes	28.26	19.23
Neutrophils	39.27	42.96
Eosinophils	17.96	6.978
cDCs	12.22	7.96
pDCs	2.193	2.167

* Cell % = cell # of a cell type x 100 / all the cell # in the condition

Figure 6

Figure 6: Single-cell RNAseq analysis reveals loss of splenic mouse and human erythroblastic macrophages in HMOX-1$^{-/-}$ HIS mice

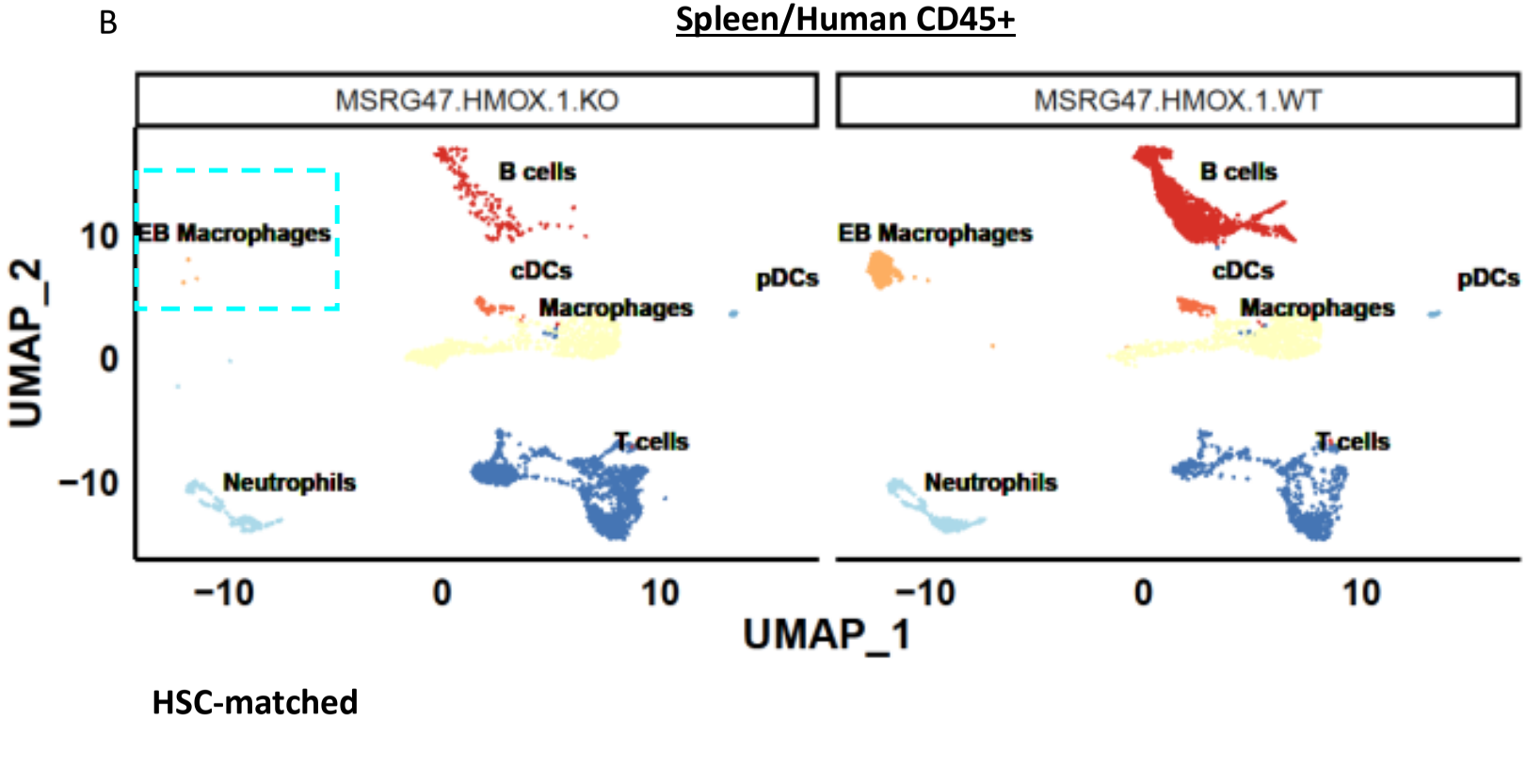

Cell %	KO	WT
EB Macrophages	0.098	11.84
Neutrophils	5.435	8.61
B cells	4.879	38.5
Macrophages	29.24	19.31
T cells	57.3	17.48
cDCs	2.227	2.994
pDCs	0.819	1.276

*** Cell % = cell # of a cell type x 100 / all the cell # in the condition**